Computer Assisted Mechanics and Engineering Sciences, 8: 501–512, 2001.

Attitude control of flexible space structures using extended state observer

Bagus Mahawan
Dynax Corporation, 1-12-7-1001, Fuchu-machi, Fuchu, Tokyo 183-0055, Japan

Zheng-Hua Luo
Dynaservo Inc., 3950 14th Avenue, Suite 402, Markham, Ontario, Canada L3R 0A9

Jing-Qing Han
Chinese Academy of Sciences, China

(Received June 1, 1999)

In this paper, we construct a nonlinear Extended State Observer (ESO) to estimate the dynamics of linear or nonlinear systems with parameter uncertainties and unknown external disturbances. We then apply ESO to the high-precision attitude control of a flexible satellite whose dynamics are unknown. Simulation results demonstrate the usefulness of the proposed control method.

Keywords: attitude control, extended state observer, flexible satellites

1. INTRODUCTION

Space structures, such as space robots, spacecrafts, and satellites, are likely to play an increasingly important role in space missions. Indeed, a large number of satellites are currently orbiting the earth.

Unlike ground-based structures for industrial use, space structures must be very lightweight, and thus tend to be very flexible. The flexibility of the structures causes elastic vibration, which in turn brings about problems in modeling and control design [6].

For a long time, linear and nonlinear control techniques have been developed for control of space structures [1, 6, 9]. In particular, the implementation of such control laws require the knowledge of the entire dynamics of the systems. Meanwhile, there has been some interests in working on the modeling and identification of the flexible space structures. Modi et al. studied the dynamics of the space station-based mobile servicing system using the Lagrangian approach [8]. In another experiment, Japan's National Space Development Agency (NASDA) carried out several in-orbit identification experiments in order to obtain the exact parameters for the model of their Engineering Test Satellite (ETS-VI) [3].

In this paper, we are interested in designing a controller for high-precision attitude control of a flexible space structure whose dynamics are unknown. The main idea is to consider the unknown dynamics of the flexible space structure including oscillation characteristics, as a new state variable, and to use an *Extended State Observer* (ESO) to estimate the new state variable for feedforward compensation. The advantages of the proposed control algorithm are twofold:

- No knowledge of the system dynamics is required in the implementation of the control law, since it can estimate the system's unknown dynamics,
- The derived control algorithm is simple, allowing us to easily implement it.

This paper is organized as follows. In Section 2, we first give an illustration of a flexible satellite as the most common example of a space structure. We then introduce the general idea of the ESO in Section 3, and also show how to design an ESO for attitude control of a flexible satellite. Simulations using the developed controller are performed, and the results will be presented in Section 4.

2. Model of a Flexible Satellite

Flexible space structures cover a wide range of mechanical structures, including flexible space stations, flexible satellites, and flexible robot arms. In this paper, we restrict our discussion to a satellite with flexible solar paddles (see Fig. 1) in order to give a more concrete illustration and to simplify our discussion. However, the discussion is also applicable to other space structures.

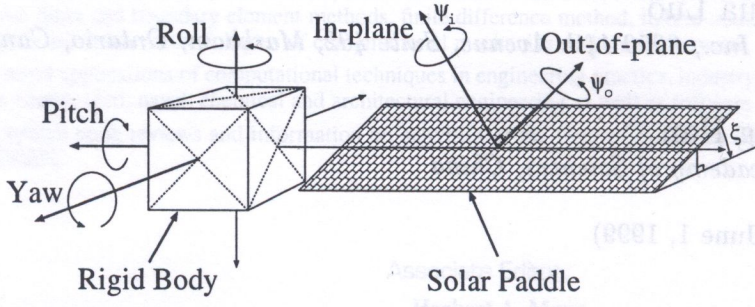

Fig. 1. Schematic diagram of a flexible satellite

Consider a flexible satellite whose schematic diagram is shown in Fig. 1. The attitude of the satellite is described by three axes, i.e., pitch, roll, and yaw. Since the structure of the satellite is symmetric, the pitch motion of the satellite is independent from those of roll and yaw. Meanwhile, roll and yaw are coupled via the solar paddles which rotate around the pitch axis. However, in a linearized approach, it is possible to eliminate the coupled motion between roll and yaw by defining *in-plane* deflection ψ_i and *out-of-plane* deflection ψ_o such as depicted in Fig. 1 (see [7, 10] for detail), so that we are able to treat the attitude control problem as three independent SISO control problems, i.e., roll, yaw, and pitch axis control problems. The transformation from in-plane and out-of-plane deflection to roll and yaw axis angular position is written as follows [3],

$$\begin{pmatrix} \phi \\ \theta \end{pmatrix} = \begin{bmatrix} \cos\xi & \sin\xi \\ -\sin\xi & \cos\xi \end{bmatrix} \begin{pmatrix} \psi_i \\ \psi_o \end{pmatrix}, \tag{1}$$

where ξ [deg] denotes the angular position of the solar paddle towards the body of the satellite, and ϕ [deg] and θ [deg] are the attitude of the satellite in the roll and yaw axis direction, respectively. Since the model for each control problem can be represented in the same manner, only the control problem for the yaw axis is considered here.

Let $u(s)$ be the control input (thruster torque), and $\theta(s)$ be the attitude in the yaw axis direction (referred hereafter to as the yaw angle), which is measurable. The transfer function from $u(s)$ to $\theta(s)$ then can be represented as the sum of n-dimension oscillation models, which is expressed in the following transfer function [2].

$$\frac{\theta(s)}{u(s)} = \frac{1}{Js^2} + \sum_{i=1}^{n} \frac{\gamma_i^2}{s^2 + 2\zeta_i\omega_i s + \omega_i^2}. \tag{2}$$

In (2), J [kg·m^2] denotes the moment inertia of the solar paddle. ζ_i, ω_i, and γ_i $(i = 1, \ldots, n)$ are, respectively, the damping coefficient, the characteristic frequency, and the torque admittance for i-th oscillation model. Particularly in the control design of satellites, the exact values of these

parameters are usually difficult to obtain. Therefore, in the next section we assume that most of the parameters are unknown, whereas the approximate values of some are known.

3. CONTROLLER DESIGN

3.1. A general extended state observer

Before we design a controller for a flexible satellite discussed in the previous section, let us give a general idea of an extended state observer [4].

Consider a nonlinear uncertain system described below:

$$x^{(n)} = f(x, \dot{x}, \ldots, x^{(n-1)}, t) + d(t) + bu(t), \tag{3}$$

where $f : [0, \infty) \times D \to \mathcal{R}$ denotes the unknown dynamics, $d : [0, \infty) \to \mathcal{R}$ and $u \in \mathcal{R}$ denote an unknown external disturbance and the input to the system respectively. $b(\neq 0) \in \mathcal{R}$ is a constant gain which is known. Assume that f, d, and u are piecewise continuous in t and locally Lipschitz in x on $[0, \infty) \times D$, and $D \in \mathcal{R}^n$. Suppose we can only measure the state $x \in \mathcal{R}$. Our question is whether we can construct an observer to estimate the unknown functions $f(\cdot) + d(t)$ by an online algorithm. For this purpose, let us define

$$a(t) = f(x, \dot{x}, \ldots, x^{(n-1)}, t) + d(t),$$

as an unknown time function, and rewrite (3) as

$$x^{(n)} = a(t) + bu(t). \tag{4}$$

An important point here is that, instead of considering $f(\cdot) + d(t)$ as a nonlinear function of x, we are considering $a(t)$ as a time function. In this way, the nonlinear equation (3) apparently becomes a time-varying equation (4). The problem now is how to estimate the time function $a(t)$. To proceed further, we define

$$\begin{cases} x_i &= x^{(i-1)}, \qquad\qquad (i = 1, \ldots, n), \\ x_{n+1} &= x^{(n)} - bu(t) = a(t). \end{cases}$$

where $x_{n+1}(= a(t))$ is referred to as an *extended state variable*. In terms of these variables, (4) is equivalent to

$$\begin{cases} \dot{x}_1 &= x_2, \\ &\vdots \\ \dot{x}_n &= x_{n+1} + bu(t), \\ \dot{x}_{n+1} &= \dot{a}(t). \end{cases} \tag{5}$$

Here, it is necessary to assume that $a(t)$ is differentiable to guarantee the existence and the boundedness of $\dot{a}(t)$. To estimate the states x_i, $(i = 1, \ldots, n+1)$, we construct a nonlinear observer

$$\begin{cases} \dot{z}_1(t) &= z_2(t) - \beta_1 g_1(\epsilon_1(t)), \\ &\vdots \\ \dot{z}_n(t) &= z_{n+1}(t) - \beta_n g_n(\epsilon_1(t)) + bu(t), \\ \dot{z}_{n+1}(t) &= = -\beta_{n+1} g_{n+1}(\epsilon_1(t)), \end{cases} \tag{6}$$

where $\epsilon_i(t) = z_i(t) - x_i(t)$, $(i = 1, \ldots, n+1)$ denote the observer's estimation errors. By this definition, we are able to rewrite (6) as follows

$$\begin{cases} \dot{\epsilon}_1(t) &= \epsilon_2(t) - \beta_1 g_1(\epsilon_1(t)), \\ &\vdots \\ \dot{\epsilon}_n(t) &= \epsilon_{n+1}(t) - \beta_n g_n(\epsilon_1(t)), \\ \dot{\epsilon}_{n+1}(t) &= -\dot{a}(t) - \beta_{n+1} g_{n+1}(\epsilon_1(t)). \end{cases} \tag{7}$$

When $\dot{a}(t)$ varies in a certain range, it is possible to choose the appropriate nonlinear functions g_i and constants β_i in (7) such that the estimation errors $\epsilon_i(t)$ are bounded as time tends to infinity, or in other words, $\epsilon(t)$ converge to the neighborhood of the origin. Therefore, $x_{n+1}(t)$ tracks the system dynamics $a(t)$, allowing us to use the estimated dynamics to compensate for the uncertainties in order to achieve good control performance.

In the next section, we show the concrete forms of the nonlinear functions in the extended state observer (6) for a flexible satellite, and we explain why they work.

3.2. ESO for a flexible satellite

Let us consider that the dynamics of the flexible satellite are written as the following second order differential equation,

$$\ddot{\theta}^*(t) = f(\theta^*, \dot{\theta}^*) + d(t) + bu(t), \tag{8}$$

where $\theta^* := J_0\theta$, and J_0 is the approximate value of J. In (8), we know only the constant J_0 and b, which are not necessarily the exact values of the plant. $f(\theta^*, \dot{\theta}^*)$ and $d(t)$ are assumed as the unknown dynamics and unknown external disturbance. As in the previous section, we define

$$a(t) := f(\theta^*, \dot{\theta}^*) + d(t)$$

as an unknown time function, then substitute this into (8) to get

$$\ddot{\theta}^*(t) = a(t) + bu(t). \tag{9}$$

Obviously, if the values of $a(t)$ can be estimated in real time, then the unknown dynamics can be compensated by the control input $u(t)$.

In what follows, we consider $a(t)$ as an extended state and we construct an ESO for (9) to estimate $a(t)$ for feedforward compensation. Specifically, the ESO is given by the following nonlinear differential equations,

$$\begin{cases} \dot{z}_1 = z_2 - \beta_1 g_1(\epsilon_1), & z_1(0) = 0, \\ \dot{z}_2 = z_3 - \beta_2 g_2(\epsilon_1) + bu, & z_2(0) = 0, \\ \dot{z}_3 = -\beta_3 g_3(\epsilon_1), & z_3(0) = 0, \end{cases} \tag{10}$$

where

$$\epsilon_1(t) = z_1(t) - \theta^*(t)$$

represents the estimation error of a quantity related to the yaw angle of the satellite. The nonlinear function $g_i(\epsilon_1)$ are chosen as

$$g_i(\epsilon_1) = \begin{cases} |\epsilon_1|^{\alpha_i} \operatorname{sign}(\epsilon_1), & |\epsilon_1| > \delta, \\ \dfrac{\epsilon_1}{\delta^{(1-\alpha_i)}}, & |\epsilon_1| \le \delta. \end{cases} \tag{11}$$

$\beta_i > 0$ and $0 < \alpha_i \leq 1$ $(i = 1,2,3)$ are prespecified design parameters, which are constants. Basically, $g_i(\epsilon_1)$ are switching functions, but to avoid chattering at $\epsilon_1 = 0$, a small constant $\delta(>0)$ is introduced. It also should be noted that due to the existence of the nonlinear term $|\epsilon_1|^{\alpha_i}$, the gain of $g_i(\epsilon_1)$ in the neighborhood of the origin is very large.

Let us put the case that $\alpha_i = 1$, $(i = 1,2,3)$, and study the stability of the ESO. First, we introduce ESO's estimation errors $\epsilon_i(t)$ $(i = 1,2,3)$ defined as

$$\epsilon_i(t) = z_i(t) - x_i(t). \tag{12}$$

Differentiating (12) and substituting (10) to the result yields the following state space representation,

$$\dot{\epsilon}(t) = A\epsilon(t) - \nu(t), \tag{13}$$

where

$$A = \begin{bmatrix} -\beta_1 & 1 & 0 \\ -\beta_2 & 0 & 1 \\ -\beta_3 & 0 & 0 \end{bmatrix}, \quad \nu(t) = \begin{pmatrix} 0 \\ 0 \\ \dot{a}(t) \end{pmatrix}, \quad \epsilon(t) = \begin{pmatrix} \epsilon_1(t) \\ \epsilon_2(t) \\ \epsilon_3(t) \end{pmatrix}.$$

We can view (13) as a perturbation of the nominal system $\dot{\epsilon}(t) = A\epsilon(t)$, with the perturbation term $\nu(t)$. When $\nu(t) = 0$, it is immediate to see that (13) is exponentially stable if and only if A is a Hurwitz matrix, that is, all eigenvalues λ_i of A satisfy Re $\lambda_i(A) < 0$. This condition can be easily satisfied by choosing

$$\beta_1\beta_2 > \beta_3\,. \tag{14}$$

We are, however, concerned with the stability of (13) when $\nu(t) \neq 0$ since $\nu(t)$ contains the derivative of the system dynamics $\dot{a}(t)$. Due to the perturbation term $\nu(t)$, the origin $\epsilon = 0$ may not be an equilibrium point of the system shown in (13). Thus, we can no longer study the stability of the origin as an equilibrium point, nor should we expect the solution of the perturbed system to approach the origin as $t \to \infty$. The best we can hope for is that if $\nu(t)$ is bounded in some sense, the $\epsilon(t)$ will be ultimately bounded by a small bound, that is, $\|\epsilon(t)\|$ will be small for sufficiently large t.

To simplify the stability analysis, we transform the system shown in (13) into the following controllable canonical form

$$\tilde{\epsilon}(t) = \tilde{A}\tilde{\epsilon}(t) - \tilde{\nu}(t), \tag{15}$$

where $\tilde{\epsilon}(t) := T\epsilon(t)$, $\tilde{\nu}(t) := T\nu(t)$, such that $\tilde{A}$ is a diagonal matrix written as $\tilde{A} := TAT^{-1} = \mathrm{diag}(\lambda_1\,,\,\lambda_2\,,\,\lambda_3)$. This can be done by defining T as

$$T := V^T = \begin{bmatrix} \lambda_1^2 & \lambda_1 & 1 \\ \lambda_2^2 & \lambda_2 & 1 \\ \lambda_3^2 & \lambda_3 & 1 \end{bmatrix},$$

where V is the Vandermonde matrix. Here, we need to assume that $\lambda_i \neq \lambda_j$, $(i \neq j)$ to guarantee the non-singularity of the transformation matrix T. Since $\tilde{A}$ is a diagonal matrix, we are now able to treat (15) as three independent state space equations, which can be rewritten as follows

$$\tilde{\epsilon}_i(t) = \lambda_i\tilde{\epsilon}_i(t) - \dot{a}(t), \qquad i = 1,2,3. \tag{16}$$

Using the convolution theorem, we see that the solution of (16) is given by

$$\tilde{\epsilon}_i(t) = -\int_0^t e^{\lambda_i(t-\tau)}\dot{a}(\tau)\,\mathrm{d}\tau. \tag{17}$$

Taking the absolute value of (17), we have

$$|\tilde{\epsilon}_i(t)| = \left| \int_0^t e^{\lambda_i(t-\tau)} \dot{a}(\tau)\, \mathrm{d}\tau \right| \leq \int_0^t \left| e^{\lambda_i(t-\tau)} \dot{a}(\tau) \right| \mathrm{d}\tau \leq \int_0^t \left| e^{\lambda_i(t-\tau)} \right| \cdot |\dot{a}(\tau)|\, \mathrm{d}\tau. \tag{18}$$

Now, let a_0 be the upper bound of $|\dot{a}(t)|$ such that

$$\sup_{t\in[0,\infty)} |\dot{a}(t)| \leq a_0\,,$$

and let $\bar{\lambda}_i$ be the real part of λ_i defined as $\bar{\lambda}_i := \mathrm{Re}[\lambda_i(A)] < 0$. Thus, (18) can be calculated as follows

$$|\tilde{\epsilon}_i(t)| \leq a_0 \int_0^t \left| e^{\bar{\lambda}_i(t-\tau)} \right| \mathrm{d}\tau \leq a_0 \left| e^{\bar{\lambda}_i t} \right| \int_0^t \left| e^{-\bar{\lambda}_i \tau} \right| \mathrm{d}\tau = \frac{a_0}{|\bar{\lambda}_i|} \left(1 - e^{\bar{\lambda}_i t} \right). \tag{19}$$

Hence, for sufficiently large t, it is obvious that

$$\lim_{t\to\infty} |\tilde{\epsilon}_i(t)| \leq \frac{a_0}{|\bar{\lambda}_i|} := b_0 \tag{20}$$

which shows that $\tilde{\epsilon}_i(t)$ are *uniformly ultimately bounded*[1]. This implies that the estimation errors $\epsilon_i(t)$ are also uniformly ultimately bounded, i.e, $\epsilon_i(t)$ converge to the neighborhood of the origin as $t \to \infty$, with the upper bound b_0. It should be noted that, since $\nu(t) \neq 0$, the estimation errors $\epsilon_i(t)$ do not converge to the origin but to the *neighborhood* of the origin instead. However, as the upper bound is inversely proportional to $|\bar{\lambda}_i|$ and $\bar{\lambda}_i$ can be arbitrarily specified by choosing proper design parameters β_i, we are able choose β_i such that $|\bar{\lambda}_i|$ is sufficiently large and thus b_0 is sufficiently small. This result can be summarized in the following theorem.

Theorem 1. *Under the condition (14), the estimation errors $\epsilon(t)$ of the system shown in (13) are ultimately bounded as $t \to \infty$, where it is possible to choose the design parameters β_i such that the upper bound b_0 is sufficiently small.*

Now, let β_i be properly specified such that the upper bound b_0 is sufficiently small, or $b_0 \to 0$. If we determine the control torque u according to

$$u(t) = u_0(t) - b^{-1} z_3(t) \tag{21}$$

where u_0 is a properly designed feedback controller, then it is obvious that

$$\ddot{\theta}^*(t) = b u_0(t)$$

which shows that the dynamic $a(t)$ is canceled, and $\ddot{\theta}^*$ depends only on $u_0(t)$. With this result, it is possible to design a controller $u_0(t)$ such that, the yaw angle $\theta(t)$ moves accurately to a given desired position. Here, $u_0(t)$ is chosen as an I-PD controller given as

$$u_0(t) = -k_p \theta(t) - k_d \dot{\theta}(t) + k_i \int_0^t e(\tau) d\tau, \tag{22}$$

where $e(t) = r - \theta(t)$ represents the yaw angular position error.

We have shown that the ESO (10) can estimate and compensate for the unknown dynamic $a(t)$, allowing us to realize high performance attitude control. This is a significant advantage since we do not need to conduct identification experiments.

[1]The general idea of the ultimately boundedness is given in [5]

4. SIMULATION RESULTS

Several simulations are conducted to verify the effectiveness of ESO. The closed loop system for simulations is shown in Fig. 2. The model for the flexible satellite is given in (2), where the order of the oscillation mode $n = 3$. The physical parameters for the model, some of which are the same as those in [3], are listed in Table 1.

For comparison, two controllers are used:

1. I-PD only, [Eq. (22)],
2. I-PD + ESO, [Eq. (22) + Eqs. (10), (21)].

The latter controller is referred hereafter to as an ESO controller. Unless otherwise specified, the various constants for both I-PD and ESO are as listed in Table 2, where α_i and β_i are determined by trial and error.

The objective of the simulations is to control the output of the closed loop system shown in Fig. 2, which is the satellite's attitude in the yaw axis direction $\theta(t)$, so that it moves from its initial position 0.0° to a given desired position +0.05°.

Simulations results are shown in Figs. 3–7. Figure 3 (top) shows the yaw angle $\theta(t)$ when the parameters of the plant are exactly known, using both controllers. The result using the I-PD is plotted with the dashed line, and the result using ESO is with the solid line. Both results show good transient response and there is no significant difference between the two controllers. This is natural since the I-PD parameters are determined such that the system gives the best result using the frequency region method [11]. However, the results become different when, for instance, the inertia J is not exactly known.

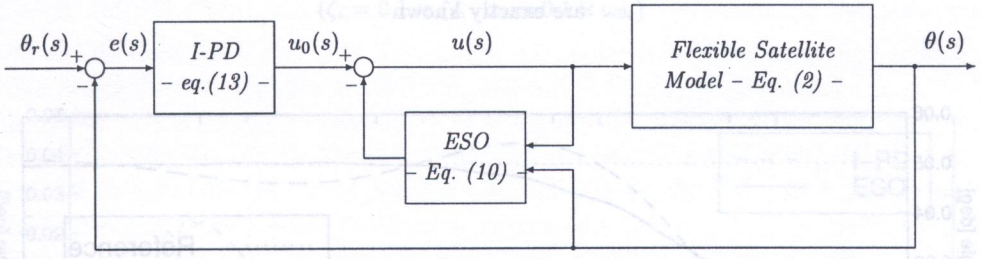

Fig. 2. Closed Loop System

Table 1. Physical parameters of the flexible satellite

Parameter	Value	Unit
Moment of Inertia	$J = 13256$	[kg·m^2/rad^2]
Torque admittance	$\gamma_1 = 0.0155$ $\gamma_2 = 0.007$ $\gamma_3 = 0.001$	
Damping coefficient	$\zeta_1 = 0.005$ $\zeta_2 = 0.01$ $\zeta_3 = 0.05$	
Characteristic frequency	$\omega_1 = 2\pi \times 0.177$ $\omega_2 = 2\pi \times 1$ $\omega_3 = 2\pi \times 10$	[rad/sec]

Table 2. I-PD and ESO parameters

Parameter	Value
I-PD feedback gain	$k_p = 69.9$ $k_i = 1.329$ $k_d = 1329$
ESO design parameters	$\alpha_1 = 1$ $\alpha_2 = 1$ $\alpha_3 = 1$ $\beta_1 = 10$ $\beta_2 = 10$ $\beta_3 = 10$ $\delta = 10^{-3}$

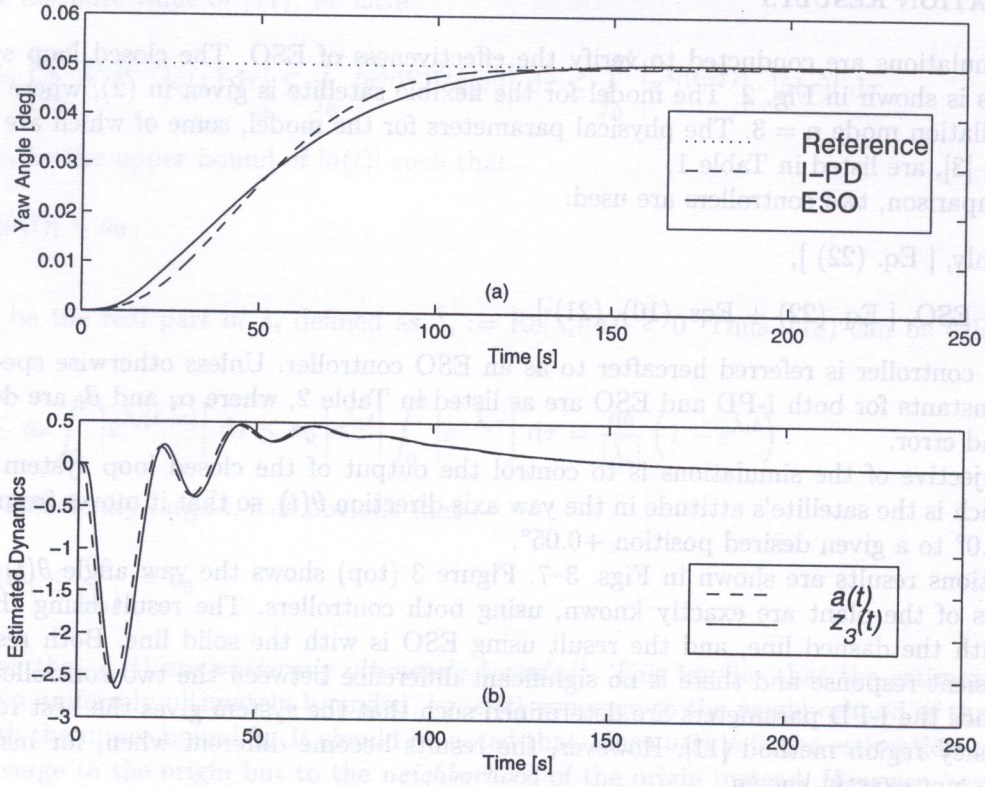

Fig. 3. Yaw angle $\theta(t)$, system dynamics $a(t)$, and its estimated value $z_3(t)$, when the plant's parameters are exactly known

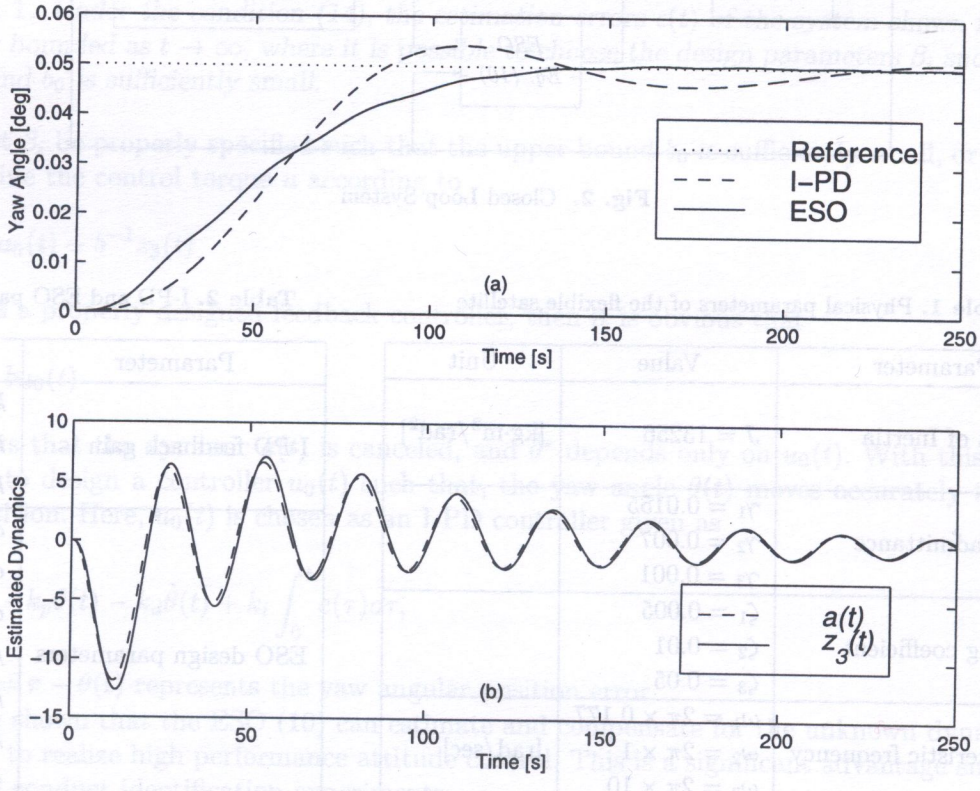

Fig. 4. I-PD and ESO comparison, when the plant's inertia are unknown ($J = 2 \times J_0$)

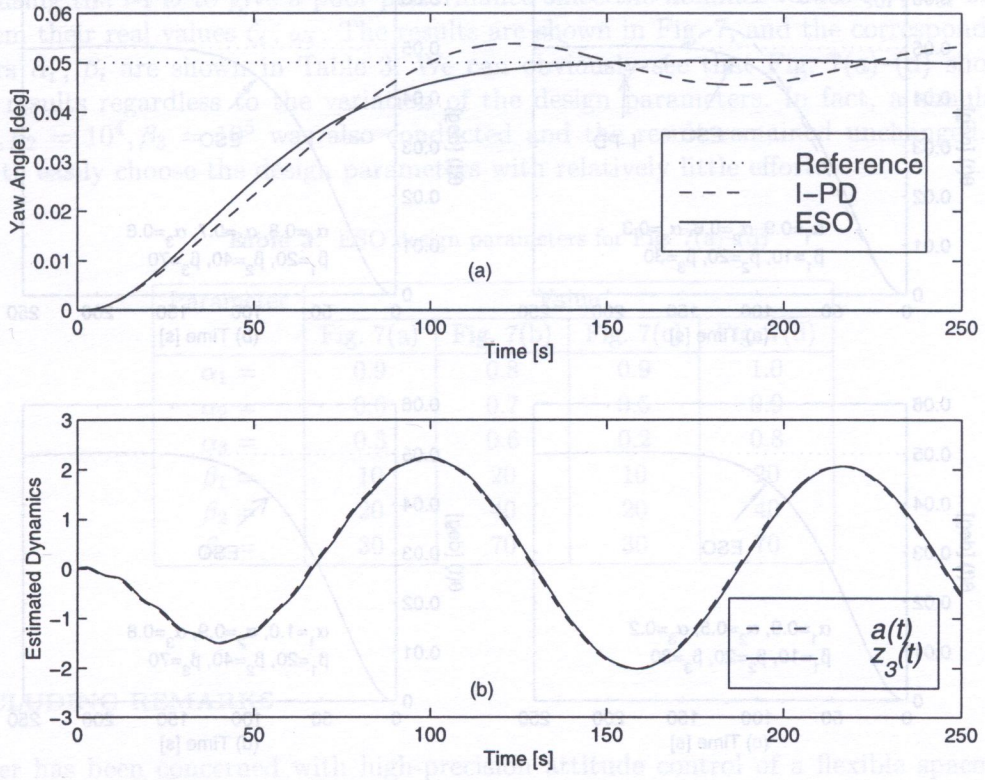

Fig. 5. I-PD and ESO comparison, when the damping ratio and the natural frequency are unknown ($\zeta_i = 0.1 \times \zeta_{0i}$, $\omega_i = 0.1 \times \omega_{0i}$)

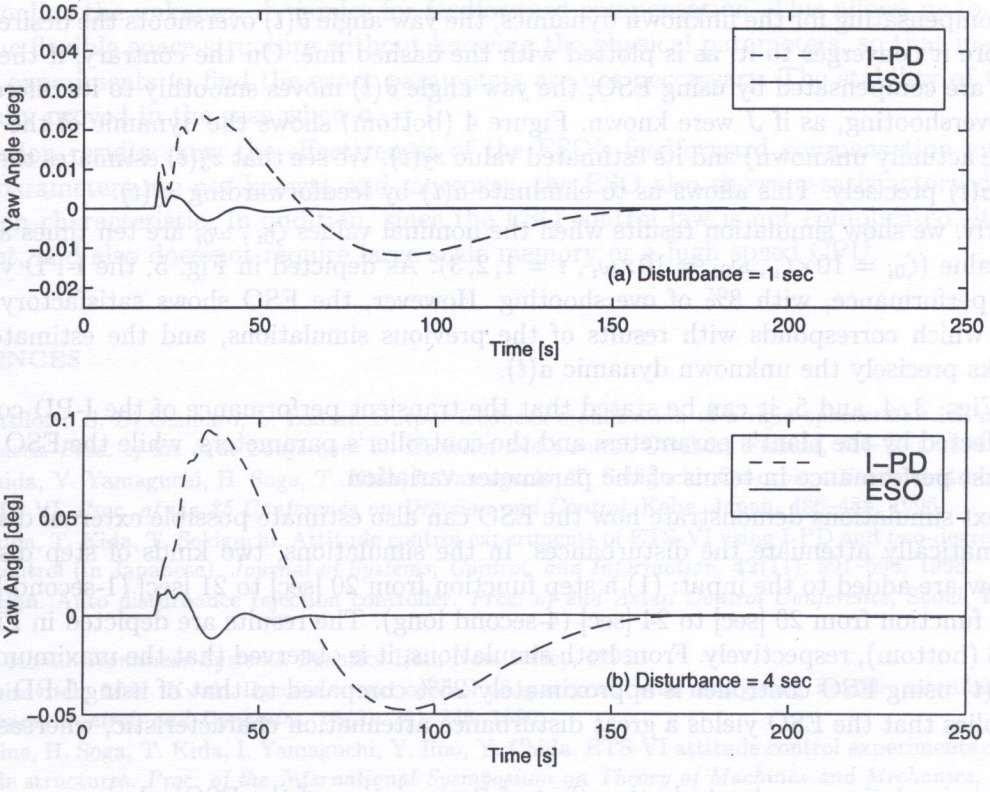

Fig. 6. Robust stability of ESO, under various disturbances

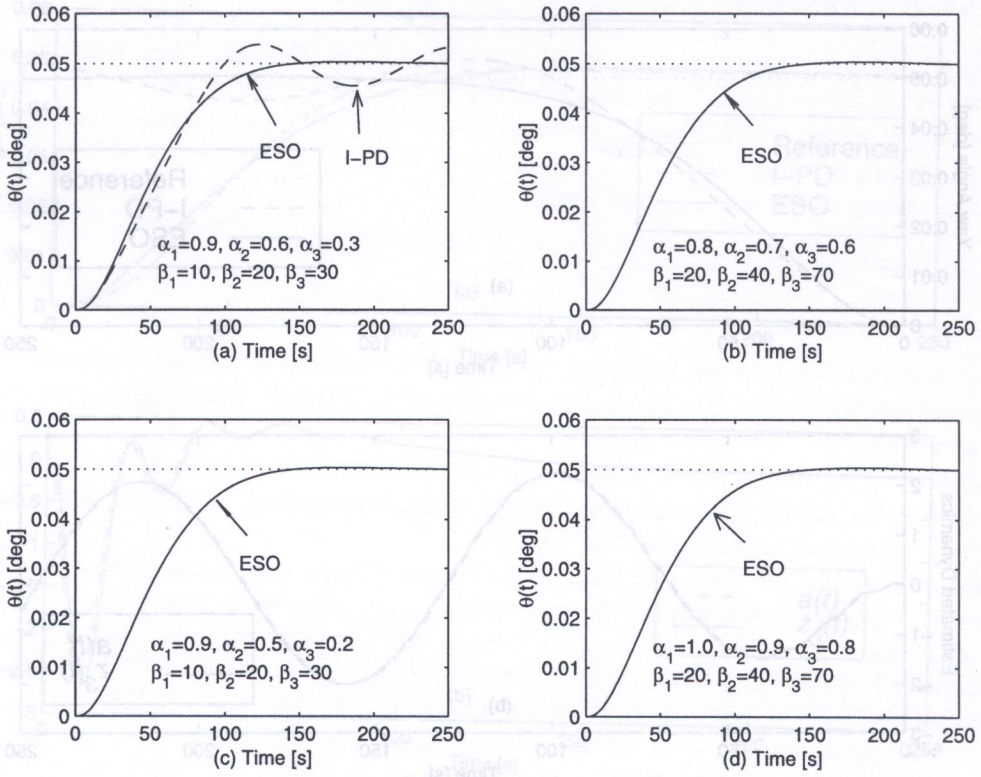

Fig. 7. System output using ESO, when the design parameters (α_i , β_i) vary

Figure 4 shows the yaw angle $\theta(t)$ when the real inertia J is twice as much as the nominal value J_0 , i.e., $J = 2{\times}J_0$. From Fig. 4 (top) we can see that, when only I-PD feedback controller is used without compensating for the unknown dynamics, the yaw angle $\theta(t)$ overshoots the desired position 0.05° before it converges to it, as is plotted with the dashed line. On the contrary, if the unknown dynamics are compensated by using ESO, the yaw angle $\theta(t)$ moves smoothly to its reference point without overshooting, as if J were known. Figure 4 (bottom) shows the dynamic of the plant $a(t)$ (which are actually unknown) and its estimated value $z_3(t)$. We see that $z_3(t)$ estimates the unknown dynamic $a(t)$ precisely. This allows us to eliminate $a(t)$ by feedforwarding $z_3(t)$.

Similarly, we show simulation results when the nominal values ζ_{0i} , ω_{0i} are ten times as much as the real value ($\zeta_{0i} = 10{\times}\zeta_i$, $\omega_{01} = 10{\times}\omega_i$, $i = 1, 2, 3$). As depicted in Fig. 5, the I-PD yields poor transient performance, with 8% of overshooting. However, the ESO shows satisfactory transient response, which corresponds with results of the previous simulations, and the estimated output $z_3(t)$ tracks precisely the unknown dynamic $a(t)$.

From Figs. 3, 4, and 5, it can be stated that the transient performance of the I-PD controller is greatly affected by the plant's parameters and the controller's parameters, while the ESO controller gives robust performance in terms of the parameter variation.

The next simulations demonstrate how the ESO can also estimate possible external disturbances and automatically attenuate the disturbances. In the simulations, two kinds of step disturbances given below are added to the input: (1) a step function from 20 [sec] to 21 [sec] (1-second long), and (2) a step function from 20 [sec] to 24 [sec] (4-second long). The results are depicted in Fig. 6 (top) and Fig. 6 (bottom), respectively. From both simulations, it is observed that the maximum displacement of $\theta(t)$ using ESO controller is approximately 25% compared to that of using I-PD controller, which implies that the ESO yields a great disturbance attenuation characteristic, whereas the I-PD does not.

The last simulations are to study the effect of the variation of the ESO's design parameters α_i , β_i to the output of the system $\theta(t)$. The plant's parameters ζ_i , ω_i are set to be the same as those of

Fig. 5, causing the I-PD to give a poor performance since the nominal values ζ_{0i}, ω_{0i} of the plant are far from their real values ζ_i, ω_i. The results are shown in Fig. 7, and the corresponding design parameters α_i, β_i are shown in Table 3. We can obviously see that Fig. 7(a)–(d) shows almost the same results regardless to the variation of the design parameters. In fact, a simulation with $\beta_1 = 10^3, \beta_2 = 10^4, \beta_3 = 10^5$ was also conducted and the result remained unchanged. This fact allows us to easily choose the design parameters with relatively little effort.

Table 3. ESO design parameters for Fig. 7(a)–(d)

Parameter	Value			
	Fig. 7(a)	Fig. 7(b)	Fig. 7(c)	Fig. 7(d)
$\alpha_1 =$	0.9	0.8	0.9	1.0
$\alpha_2 =$	0.6	0.7	0.5	0.9
$\alpha_3 =$	0.3	0.6	0.2	0.8
$\beta_1 =$	10	20	10	20
$\beta_2 =$	20	40	20	40
$\beta_3 =$	30	70	30	70

5. Concluding remarks

This paper has been concerned with high-precision attitude control of a flexible space structure, where the dynamic model of the flexible space structure is represented as a second order nonlinear differential equation. The physical parameters involved in the dynamic model considered in this paper are not necessarily known.

By viewing the unknown dynamics as a new state and by constructing an ESO, we are able to estimate online the unknown dynamics for feedforward compensation. This allows us to accurately control the flexible space structure without knowing the physical parameters, so that in-orbit identification experiments to find the exact parameters are not neccessary. The stability of the ESO is theoritically proved in the case when $\alpha_i = 1$.

Simulation results show the effectiveness of the ESO's feedforward compensation even though the real parameters are not known, and moreover, the ESO also shows a satisfactory disturbance attenuation characteristic. In addition, since the ESO control law is not complicated, it is easy to implement, and also does not require large scale memory or a high speed CPU.

References

[1] S. Battilotti, S. Di Gennaro, L. Lanari. Output feedback stabilization of a rigid spacecraft with unknown disturbances. *Proc. of the 34th Conference on Decision and Control*, Orlando, Florida, 916–920, 1994.

[2] Y. Chida, Y. Yamaguchi, H. Soga, T. Kida, I. Yamaguchi, T. Sekiguchi. On-orbit attitude control experiments for ETS-VI. *Proc. of the 35 Conference on Decision and Control*, Kobe, Japan, 486–488, 1996.

[3] Y. Chida, T. Kida, T. Sekiguchi. Attitude control experiments of ETS-VI using I-PD and two-degree-of-freedom H^∞ control (in Japanese). *Journal of Systems, Control, and Information*, **42**(11): 591–598, 1998.

[4] J.Q. Han. Auto disturbance rejection controller. *Proc. of 2nd Asian Control Conference*, Seoul, **III**: 567–570, 1997.

[5] H. K. Khalil. *Nonlinear Systems*. Prentice Hall, New Jersey, 1996.

[6] L. Meirovitch, M.K. Kwak. Dynamics and control of spacecraft with retargeting flexible antennas. *Journal of Guidance, Control, and Dynamics*, **13**(2): 241–248, 1990.

[7] M. Mine, H. Soga, T. Kida, I. Yamaguchi, Y. Iino, Y. Chida. ETS-VI attitude control experiments on orbit with flexible structures. *Proc. of the International Sysmposium on Theory of Machines and Mechanics*, 1992.

[8] V.J. Modi, A.C. Ng, F. Karray. Slewing dynamics and control of the space station-based mobile servicing system. *Acta Astronautica*, **35**(2/3): 119–129, 1995.

[9] S. Monaco, D. Normand-Cyrot, S. Stornelli. Multirate three axes attitude stabilization of spacecraft. *Proc. of the 28th Conference on Decision and Control*, Tampa, Florida, 797–802, 1989.

[10] M. Shigehara. *Introduction to Space Engineering: Control of Satellite and Missile* (in Japanese). Baifukan, Tokyo, 1994.

[11] T. Shigemasa, et al. Two degrees of freedom PID auto-tuning controller based on frequency region methods. In: *Adaptive Control Strategies for Industrial Use*, Springer-Verlag, 349–360, 1988.

[12] S.N. Singh. Robust nonlinear attitude control of flexible spacecraft. *IEEE Trans. on Aerospace and Electronic Systems*, **AES-23**(3): 380–387, 1987.